# Interfacial Microstructures and Thermodynamics of Thermosonic Cu-Wire Bonding

Junhui Li, Linggang Liu, Luhua Deng, Bangke Ma, Fuliang Wang, and Lei Han

***Abstract*—The interfacial microstructures of the Cu-wire bonding to an Al pad are investigated first by using an X-ray microdiffractometer and high-resolution transmission electron microscopy. It was found that the intermetallic compounds hardly formed at the Cu/Al interface during the thermosonic Cu-wire bonding process. However, when heating temperature is elevated to 340 °C which increases energy levels of Cu/Al, the intermetallic phases $Al_2Cu$ and $Al_4Cu_9$ can form and reach to 130 nm thick within 20 ms due to atomic interdiffusion and reaction activated by ultrasonic energy and heat at the Cu/Al interface. The Al side of the interface is aluminum-rich $Al_2Cu$ with lattice parameters $a = 6.067$ Å and $c = 4.864$ Å, and the Cu side is copper-rich $Al_4Cu_9$ with lattice parameter $a = 8.706$ Å. Bonding strength and bondability increase significantly after forming the Cu/Al intermetallic phases.**

***Index Terms*—Bonding interface, bonding strength, Cu-wire bonding, intermetallic compounds (IMCs).**

## I. Introduction

THERE IS growing interest in copper (Cu)-wire bonding for high-speed devices and fine-pitch microelectronic applications due to significant cost saving and superior mechanical and electrical properties [1]–[3]. Cu-wire bonding may prove a potential alternative to Au-wire bonding [4], [5]. However, it is a complex process, and the physics behind it has not been fully understood. Many attempts focused on the characterization of the Cu/Al bonding interface [6], [7]. Kim *et al.* [8] have found that, after aging for 100 h at 250 °C, the Cu/Al intermetallic compound (IMC) was approximately 1.2 $\mu$m. Cu/Al IMCs in the initial bonds remain poorly understood because it is difficult to detect the Cu/Al IMCs in extremely thin alloy domains [9], [10]. Murali *et al.* [11] and Ratchev *et al.* [12] found no Cu/Al IMCs at the as-bonded state by using scanning electron microscopy. Xu *et al.* [13] and Hang *et al.* [14] also believed that no Cu/Al IMCs formed within such a short time (20–30 ms) during the bonding process. Recently, $Al_2Cu$ IMCs have been detected by Xu *et al.* [15], [16] with high-resolution transmission electron microscopy (HRTEM), and the quantity of $Al_2Cu$ increased with the increase in the levels of ultrasonic power. Therefore, this study was undertaken to examine the effect of thermal energy on interfacial characteristics of bonds which were investigated first by using an X-ray microdiffractometer. The relationship between interfacial microstructures, thermodynamics condition, and bonding strength is established.

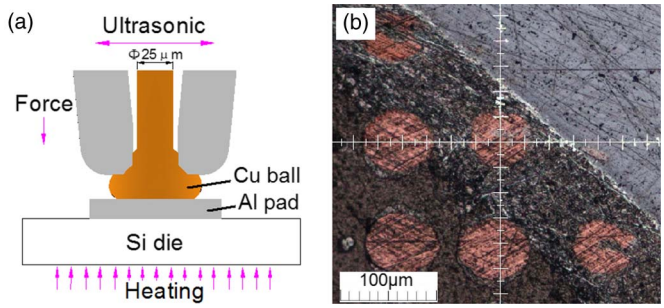


Fig. 1. (a) Test vehicle of Cu-wire bonding. (b) X-ray analysis location with the partially revealed bonding interface form.

## II. Experiment

A Cu wire (25.4-$\mu$m diameter) was ball bonded to an Al pad (2.8 $\mu$m thick) on a silicon (Si) die as shown in Fig. 1(a) by using a K&S 8028 wire bonder. Bonding was completed within 20 ms by using a combination of 150-mA ultrasonic current, 200 °C heating temperature, and 60-gf (1 gf = 9.8 mN) bonding force.

X-ray diffraction spectra of the lattice structure are like one's fingerprint and can give more precise microstructure parameters than HRTEM. To carry out X-ray diffraction testing, a sample with Cu-ball bonds was embedded in the resins and was ground carefully until the Cu/Al bonding interface was found as shown in Fig. 1(b). Then, the sample was performed with a Rigaku RAPID X-ray microdiffractometer at 48-kV voltage, 50-$\mu$m beam size, and 60-min exposure time.

To study the interfaces in detail, HRTEM sections of the Cu/Al interfaces were prepared by embedding in the epoxy, punching, grinding, and ion-sputter thinning. Then, the Cu/Al section features were observed by using F30 HRTEM with EDX in scanning (S) TEM mode at 300 kV.

## III. Results and Discussion

Fig. 2(a) shows the X-ray microdiffraction (XRD) patterns of the Cu/Al bonding. Compared with peaks of the Joint Committee on Powder Diffraction Standards database, all diffraction

Manuscript received June 2, 2011; revised June 29, 2011; accepted July 4, 2011. Date of publication August 14, 2011; date of current version September 28, 2011. This work was supported in part by the National Natural Science Foundation of China under Grant 50975292, by the China High-Technology R&D Program (973 Program) under Grant 2009CB724203, by the National S&T Major Project of China under Grant 2009ZX02038-001, and by the Program for New Century Excellent Talents in University under Grant NCET-08-0575. The review of this letter was arranged by Editor C.-P. Chang.

J. Li is with the State Key Laboratory of High Performance Complex Manufacturing and the School of Mechanical and Electrical Engineering, Central South University, Changsha 410083, China (e-mail: lijunhui@csu.edu.cn).

L. Liu, L. Deng, B. Ma, F. Wang, and L. Han are with the State Key Laboratory of High Performance Complex Manufacturing, Changsha, 410083, China (e-mail: liulinggang@163.com; dengluhua@163.com; mabangke@163.com; wangfuliang@csu.edu.cn; leihan@csu.edu.cn).

Color versions of one or more of the figures in this letter are available online at http://ieeexplore.ieee.org.

Digital Object Identifier 10.1109/LED.2011.2161749

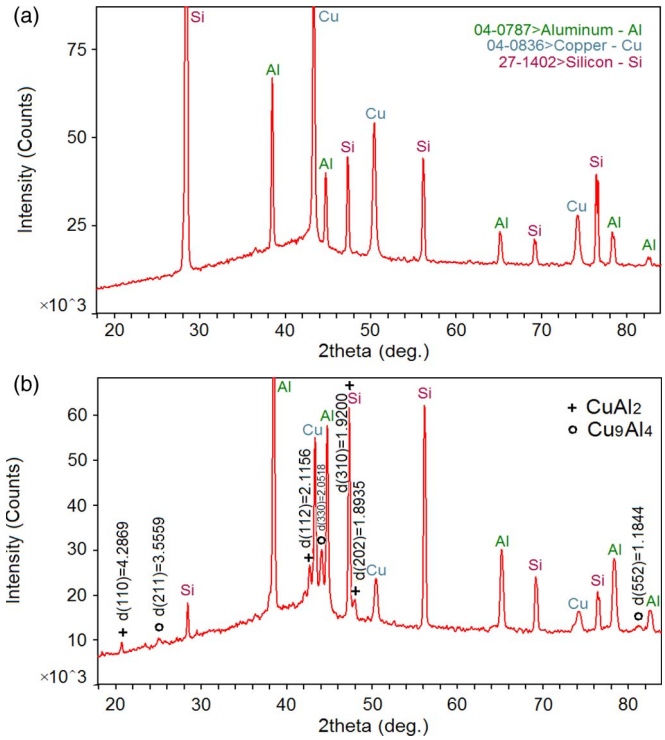


Fig. 2. XRD patterns of the Cu/Al bonding sample. (a) At 200 °C heating temperature. (b) At 340 °C heating temperature.

TABLE I
ATOMIC PROPERTIES OF Cu, Au, AND Al [11], [14]

| Properties | Cu | Au | Al |
|---|---|---|---|
| Atomic radius (Å) | 1.28 | 1.44 | 1.43 |
| Electroegativity | 2.2 | 3.1 | 1.5 |

peaks are derived from Cu, Al, and Si, and no Cu/Al IMC peaks are detected. X-ray diffraction for five samples at 200 °C shows the same diffraction peaks.

The atomic properties of the elements (i.e., Cu, Au, and Al) as shown in Table I can be used to explain why making the formation of Cu/Al IMCs is much more difficult than that of Au/Al IMCs which are $Al_2Au$, $AlAu_4$, or $Al_3Au_8$ IMCs found easily by Li *et al.* [17], Xu *et al.* [18], and Ji *et al.* [19]. Compared to Au atoms, Cu atoms have a greater atomic size misfit in the aluminum lattice and a lower electronegativity, which then hinder the formation of Cu/Al IMCs which are absent in the case of Cu bonds. At a certain thermal aging temperature, Xu *et al.* [20] revealed that the combined activation energy of Cu/Al IMC growth is 97.1 kJ/mol which is much higher than that of Au/Al IMC growth (only 40.1 kJ/mol). Making IMCs is sensitive to thermal energy.

High-frequency ultrasonic vibration led to the big acceleration about 80 000 times the acceleration of gravity by testing with a PSV-400-M2 laser vibrometer. The strong mechanical effect generates dislocations which perform the fast diffusion channels [21], and bonding was achieved rapidly at lower temperature. Although ultrasonic energy plays an important role in wire bonding, great vibration displacement driven by high ultrasonic power results in the damage of bonds and dies [22]. Therefore, the increase in heating temperature should be a better way to form the Cu/Al IMCs than ultrasonic energy.

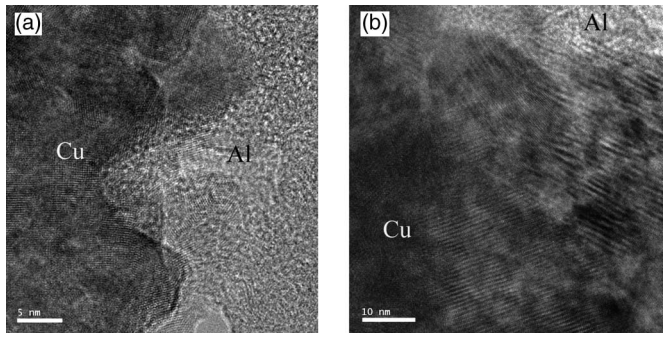


Fig. 3. Cross-sectional HRTEM image of the Cu/Al bonding interface. (a) At 200 °C heating temperature. (b) At 340 °C heating temperature.

IMC peaks were not still observed until 300 °C heating temperature, but at 340 °C, a few new diffraction peaks seen at the black circle and plus markers appear in Fig. 2(b). Crystal interplanar spacings $d_{(hkl)}$ of new diffraction peaks are listed, respectively. $(hkl)$ represents Miller indices of the crystallographic planes. Matching the micro-XRD results to the standard diffraction data, it is clear that the new peaks listed by $d_{(310)} = 1.9200$ Å, $d_{(112)} = 2.1156$ Å, $d_{(110)} = 4.2869$ Å, and $d_{(202)} = 1.8935$ Å agree well with the characteristics of $Al_2Cu$. Its lattice parameters are calculated as $a = 6.067$ Å and $c = 4.864$ Å, belonging to space group I4/mcm. Xu *et al.* [15], [16] also found IMCs $Al_2Cu$ by a Fourier-reconstructed pattern obtained from an HRTEM lattice image. The other phase with the new peaks listed by $d_{(330)} = 2.0518$ Å, $d_{(552)} = 1.1844$ Å, and $d_{(211)} = 3.5559$ Å is confirmed to be $Al_4Cu_9$. Its lattice parameter is $a = 8.706$ Å, belonging to space group $P\bar{4}3m$. Similar peaks appear for all five measured samples at 340 °C.

Typical microcharacteristics after forming Cu/Al IMCs are found in the HRTEM image as shown in Fig. 3(b), and they are different from that before forming Cu/Al IMCs as shown in Fig. 3(a). Among the various features in Fig. 3(b), some parallel interference structures with alternate dark and bright bars may present the microstructures of Cu/Al IMCs, and their intervals are regular. Two Cu/Al IMCs may be distinguished by two different intervals seen in the HRTEM image.

The features of the interdiffusion at the Cu/Al IMC interface are further analyzed by the STEM-EDX results as shown in Fig. 4. The thickness of atom diffusion at the Cu/Al interface is about 130 nm, and mesophase features are displayed. It is believed that the mesophase is related to $Al_2Cu$ and $Al_4Cu_9$, and the aluminum-rich alloy $(Al_2Cu)$ should be at the Al side of the interface with low Cu counts, while the copper-rich alloy $(Al_4Cu_9)$ should be at the Cu side. Thus, it is reasonable to believe that the microstructure with bigger intervals in Fig. 3(b) is indicated as $Al_2Cu$, and another with smaller intervals is $Al_4Cu_9$.

According to Fick's law of diffusion, Xu *et al.* [13], based on their thermal aging experimental data, concluded that the relationship between the Cu/Al IMC thickness $X$ and the time $t$ at a given temperature $T$ can be represented by

$$\chi = \left[1.2055 \times 10^{-7} \times t \times \exp\left(\frac{-11679.1}{T}\right)\right]^{1/2}. \quad (1)$$

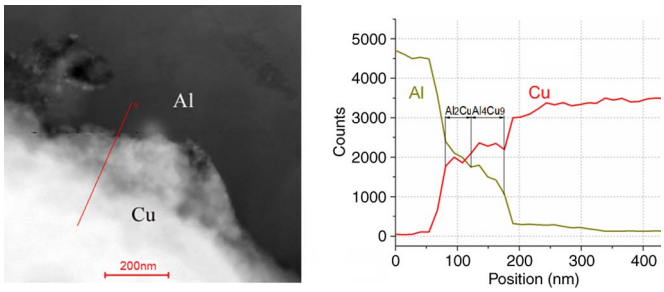


Fig. 4. STEM image and results of EDX line scanning on the cross section of the Cu/Al interface.

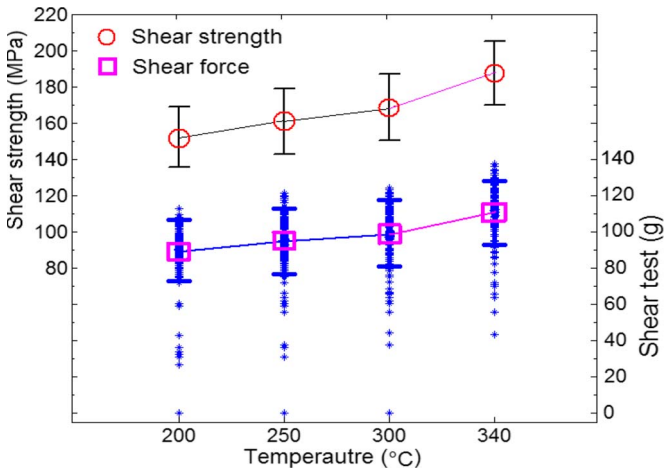


Fig. 5. Shear force and shear strength distribution map from 200 °C to 340 °C heating temperature.

Consequently, in the present studies with the IMC thickness $X = 130$ nm and the bonding time $t = 20$ ms, the temperature $T$ is estimated to be 711 °C. This temperature is too high to be reached. However, the thermal energy at 340 °C increases energy levels of Cu/Al; on the other hand, ultrasonic effect not only induces the fast atomic diffusion along high density dislocation [21] but also increases the local temperature with the previous measurement of the interfacial temperature rising from 80 °C to 120 °C measured by a K-type thermocouple microsensor [23]. Thus, Cu/Al IMCs formed due to interdiffusion and reaction activated by the combined effect of ultrasonic energy and heat at the Cu/Al bond interface.

In order to understand the effect of Cu/Al IMCs, 360 bonds were tested at various temperatures. Strength data are shown in Fig. 5. It indicates statistically the average value and standard deviations of shear force and shear strength for different temperatures. The average shear strength and bondability are significantly enhanced after the formation of the Cu/Al IMCs. IMCs increase the bonding strength by alloying between copper wires with aluminum pads.

## IV. Conclusion

The intermetallic phases cannot be found at the Cu/Al interface until heating temperature is elevated to 340 °C. The IMCs $Al_2Cu$ and $Al_4Cu_9$ can form at 340 °C within a short time (20 ms) due to diffusion and reaction activated by thermal energy combined with ultrasonic energy. Bonding strength and bondability increase significantly when the Cu/Al IMCs form.

## References

[1] H. Xu, C. Liu, V. V. Silberschmidt, Z. Chen, and J. Wei, "Initial bond formation in thermosonic gold ball bonding on aluminium metallization pads," *J. Mater. Process. Technol.*, vol. 210, no. 8, pp. 1035–1042, Jun. 2010.

[2] U. Geißler, M. Schneider-Ramelow, and H. Reichl, "Hardening and softening in AlSi bond contacts during ultrasonic wire bonding," *IEEE Trans. Compon. Packag. Technol.*, vol. 32, no. 4, pp. 794–799, Dec. 2009.

[3] S. Khoury, D. J. Burkhard, and T. A. Scharr, "A comparison of copper and gold wire bonding on integrated circuit devices," *IEEE Trans. Compon., Hybrids, Manuf. Technol.*, vol. 13, no. 4, pp. 673–681, Dec. 1990.

[4] B. I. Noh, J. M. Koo, J. L. Jo, and S. B. Jung, "Application of underfill for flip-chip package using ultrasonic bonding," *Jpn. J. Appl. Phys.*, vol. 47, no. 5, pp. 4257–4261, May 2008.

[5] Y. H. Tian, C. Q. Wang, I. Lum, M. Mayer, J. P. Jung, and Y. Zhou, "Investigation of ultrasonic copper wire wedge bonding on Au/Ni plated Cu substrates at ambient temperature," *J. Mater. Process. Technol.*, vol. 208, no. 1–3, pp. 179–186, Nov. 2008.

[6] Y. H. Tian, C. Q. Wang, and J. P. Zhao, "Reliability and failure analysis of fine copper wire bonds encapsulated with commercial epoxy molding compound," *Microelectron. Reliab.*, vol. 51, no. 1, pp. 157–165, Jan. 2011.

[7] K. Toyozawa, K. Fujita, S. Minamide, and T. Maeda, "Development of copper wire bonding application technology," *IEEE Trans. Compon., Hybrids, Manuf. Technol.*, vol. 13, no. 4, pp. 667–672, Dec. 1990.

[8] H. Kim, J. Y. Lee, and K. W. Koh, "Effects of Cu/Al intermetallic compound (IMC) on copper wire and aluminum pad bondability," *IEEE Trans. Compon. Packag. Technol.*, vol. 26, no. 2, pp. 367–374, Jun. 2003.

[9] S. Murali and C. J. Vath, III, "Effect of wire size on the formation of intermetallics and Kirkendall voids on thermal aging of thermosonic wire bonds," *Mater. Lett.*, vol. 58, no. 25, pp. 3096–3101, Oct. 2004.

[10] H. Xu, C. Liu, V. V. Silberschmidt, and Z. Chen, "Growth of intermetallic compounds in thermosonic copper wire bonding on aluminum metallization," *J. Electron. Mater.*, vol. 39, no. 1, pp. 124–131, Jan. 2010.

[11] S. Murali, N. Srikanth, and C. J. Vath, III, "An analysis of intermetallics formation of gold and copper ball bonding on thermal aging," *Mater. Res. Bull.*, vol. 38, no. 4, pp. 637–646, Mar. 2003.

[12] P. Ratchev, S. Stoukatch, and B. Swinnen, "Mechanical reliability of Au and Cu wire bonds to Al, Ni/Au and Ni/Pd/Au capped Cu bond pads," *Microelectron. Reliab.*, vol. 46, no. 8, pp. 1315–1325, Aug. 2006.

[13] H. Xu, C. Wang, and C. Hang, "Growth behaviour of intermetallic compound on bonding joint of Cu wire on Al alloy pad during thermal aging," *Acta Metall. Sin.*, vol. 43, no. 2, pp. 125–130, 2007.

[14] C. J. Hang, C. Q. Wang, M. Mayer, Y. H. Tian, Y. Zhou, and H. H. Wang, "Growth behavior of Cu/Al intermetallic compounds and cracks in copper ball bonds during isothermal aging," *Microelectron. Reliab.*, vol. 48, no. 3, pp. 416–424, Mar. 2008.

[15] H. Xu, C. Liu, Z. Chen, and V. L. Acoff, "Effect of ultrasonic energy on nanoscale interfacial structure in copper wire bonding on aluminium pads," *J. Phys. D, Appl. Phys.*, vol. 44, no. 14, p. 145 301, Apr. 2011.

[16] H. Xu, C. Liu, S. S. Pramana, T. J. White, and Z. Chen, "A re-examination of the mechanism of thermosonic copper ball bonding on aluminium metallization pads," *Scr. Mater.*, vol. 61, no. 2, pp. 165–168, Jul. 2009.

[17] J. Li, J. Duan, and J. Zhong, "Microstructural characteristics of Au/Al bonded interfaces," *Mater. Charact.*, vol. 58, no. 2, pp. 103–107, Feb. 2007.

[18] H. Xu, C. Liu, S. S. Pramana, T. J. White, Z. Chen, M. Sivakumar, and V. L. Acoff, "A micromechanism study of thermosonic gold wire bonding on aluminium pad," *J. Appl. Phys.*, vol. 108, no. 11, p. 113 517, Dec. 2010.

[19] H. Ji, M. Li, J. Kim, D. Kim, and C. Wang, "Nano features of Al/Au ultrasonic bond interface observed by high resolution transmission electron microscopy," *Mater. Charact.*, vol. 59, no. 10, pp. 1419–1424, Oct. 2008.

[20] H. Xu, C. Liu, V. V. Silberschmidt, Z. Chen, J. Wei, and M. Sivakumar, "Effect of bonding duration and substrate temperature in copper ball bonding on aluminium pads: A TEM study of interfacial evolution," *Microelectron. Reliab.*, vol. 51, no. 1, pp. 113–118, Jan. 2011.

[21] J. Li, L. Han, and J. Zhong, "Interface mechanism of ultrasonic flip chip bonding," *Appl. Phys. Lett.*, vol. 90, no. 24, p. 242 902, Jun. 2007.

[22] J. Li, L. Han, and J. Zhong, "Observations on HRTEM features of thermosonic flip chip bonding interface," *Mater. Chem. Phys.*, vol. 106, no. 2/3, pp. 457–460, Dec. 2007.

[23] P. Schwaller, P. Gröning, A. Schneuwly, P. Boschung, E. Müller, M. Blanc, and L. Schlapbach, "Surface and friction characterization by thermoelectric measurements during ultrasonic friction processes," *Ultrasonics*, vol. 38, no. 1–8, pp. 212–214, Mar. 2000.